4.6 Some Properties of the 2-D Discrete Fourier Transform

Relationships between Spatial and Frequency Intervals

Suppose that a continuous function $f(t,z)$ is sampled to form a digital image $f(x,y)$, consisting of $M \times N$ samples taken in the t- and z-directions. Let ΔT and ΔZ denote the separations between samples, then, the separations between the corresponding discrete, frequency domain variables are given by

$$\Delta u = \frac{1}{M\Delta T} \tag{4.6-1}$$

and

$$\Delta v = \frac{1}{N\Delta Z}\,. \tag{4.6-2}$$

Translation and Rotation

The Fourier transform pair satisfies the following translation properties:

$$f(x,y)e^{j2\pi(u_0 x/M + v_0 y/N)} \Leftrightarrow F(u-u_0, v-v_0) \tag{4.6-3}$$

and

$$f(x-x_0, y-y_0) \Leftrightarrow F(u,v)e^{-j2\pi(x_0 u/M + y_0 v/N)} \tag{4.6-4}$$

Using the polar coordinates

$$x = r\cos\theta \quad y = r\sin\theta \quad u = \omega\cos\varphi \quad v = \omega\sin\varphi\,,$$

we have the following transform pair:

$$f(r,\theta+\theta_0) \Leftrightarrow F(\omega,\varphi+\theta_0)\,. \tag{4.6-5}$$

Equation (4.6-5) indicates that rotating $f(x,y)$ by an angle θ_0 will rotate $F(u,v)$ by the same angle. Conversely, rotating $F(u,v)$ will rotate $f(x,y)$ by the same angle.

Periodicity

As in the 1-D case, the 2-D Fourier transform and its inverse are infinitely periodic in the u and v directions:

$$F(u,v) = F(u + k_1 M, v) = F(u, v + k_2 N) = F(u + k_1 M, v + k_2 N) \quad (4.6\text{-}6)$$

and

$$f(x,y) = f(x + k_1 M, y) = f(x, y + k_2 N) = f(x + k_1 M, y + k_2 N) \quad (4.6\text{-}7)$$

where k_1 and k_2 are integers.

The periodicities of the transform and its inverse are important issues in the implementation of DFT-based algorithms.

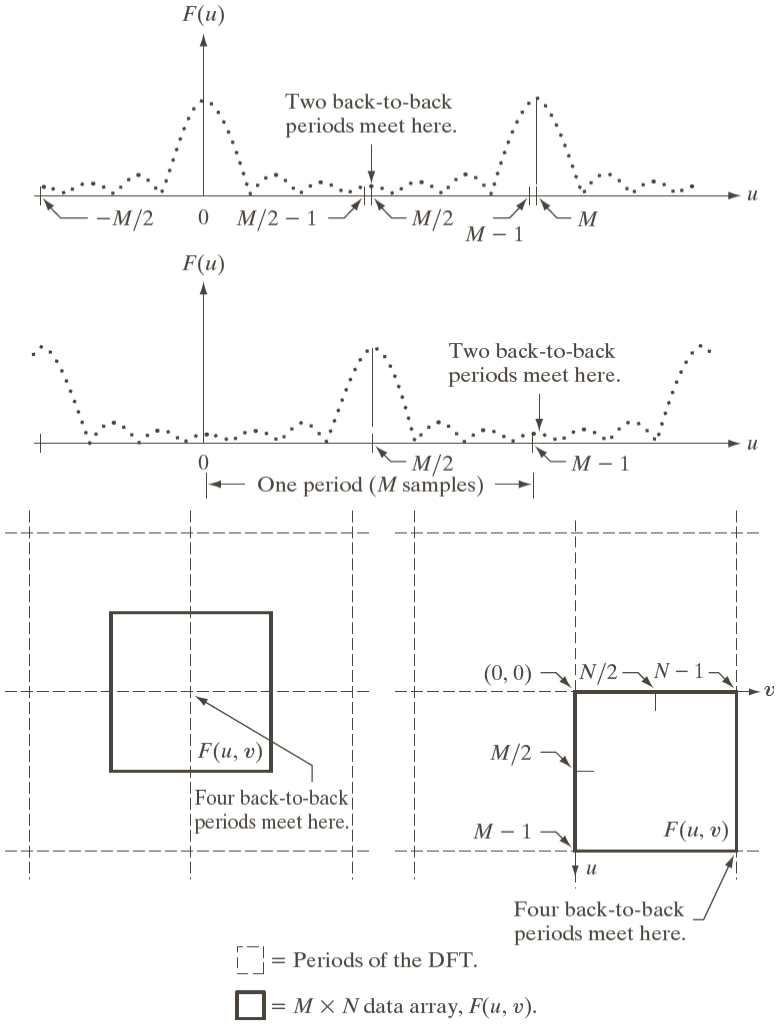

a
b
c d

FIGURE 4.23 Centering the Fourier transform. (a) A 1-D DFT showing an infinite number of periods. (b) Shifted DFT obtained by multiplying $f(x)$ by $(-1)^x$ before computing $F(u)$. (c) A 2-D DFT showing an infinite number of periods. The solid area is the $M \times N$ data array, $F(u, v)$, obtained with Eq. (4.5-15). This array consists of four quarter periods. (d) A Shifted DFT obtained by multiplying $f(x, y)$ by $(-1)^{x+y}$ before computing $F(u, v)$. The data now contains one complete, centered period, as in (b).

Considering Figure 4.23 (b) and referring to

$$f(x,y)e^{j2\pi(u_0x/M+v_0y/N)} \Leftrightarrow F(u-u_0,v-v_0), \qquad (4.6\text{-}3)$$

it follows

$$f(x)e^{j2\pi(u_0x/M)} \Leftrightarrow F(u-u_0),$$

which indicates that multiplying $f(x)$ by the exponential term will show the shifting. If we let $u_0 = M/2$, the exponential term becomes $e^{j\pi x}$, which is equal to $(-1)^x$. It follows

$$f(x)(-1)^x \Leftrightarrow F(u-M/2).$$

It means that multiplying $f(x)$ by $(-1)^x$ shits the data so that $F(0)$ is at the center of the interval $[0, M-1]$.

In a case of 2D, if we let $(u_0, v_0) = (M/2, N/2)$ in

$$f(x,y)e^{j2\pi(u_0x/M+v_0y/N)} \Leftrightarrow F(u-u_0,v-v_0), \qquad (4.6\text{-}3)$$

it will result the expression

$$f(x,y)(-1)^{x+y} \Leftrightarrow F(u-M/2,v-N/2) \qquad (4.6\text{-}8)$$

Using (4.6-8) shifts the data so that $F(0,0)$ is at the center of the frequency rectangle defined in Figure 4.23 (d).

Symmetry Properties

An important result from functional analysis is that any real or complex function, $w(x,y)$, can be expressed as the sum of an even and an odd part:

$$w(x,y) = w_e(x,y) + w_o(x,y) \qquad (4.6\text{-}9)$$

where

$$w_e(x,y) \triangleq \frac{w(x,y) + w(-x,-y)}{2} \qquad (4.6\text{-}10a)$$

and

$$w_o(x,y) \triangleq \frac{w(x,y) - w(-x,-y)}{2}. \qquad (4.6\text{-}10b)$$

It follows that

$$w_e(x,y) = w_e(-x,-y) \qquad (4.6\text{-}11a)$$

and

$$w_o(x,y) = -w_o(-x,-y) \qquad (4.6\text{-}11b)$$

Even functions are said to be symmetric and odd functions are antisymmetric.

Since all indices in DFT and IDFT are positive, when we say "symmetry (antisymmetry)" we are referring to symmetry (antisymmetry) about the center point of a sequence.

It is more convenient to think only in terms of nonnegative indices, in which case

$$w_e(x,y) = w_e(M-x, N-y) \qquad (4.6\text{-}12a)$$

and

$$w_o(x,y) = -w_o(M-x, N-y) \qquad (4.6\text{-}12b)$$

where M and N are the number of rows and columns of a 2-D array.

We know that the product of two even or odd functions is even, and the product of an even and an odd is odd. In addition, the only way that a discrete function can be odd is if all its samples sum to zero.

These lead to the important result of

$$\sum_{x=0}^{M-1}\sum_{y=0}^{N-1} w_e(x,y)w_o(x,y) = 0 \,. \qquad (4.6\text{-}13)$$

In other words, because the argument of (4.6-13) is odd, the result of the summations is 0. the functions can be real or complex.

Example 4.10: Even and odd functions

The evenness and oddness of discrete sequences are not as easy to visualize as those of continuous functions. Consider the 1-D sequence

$$f = \{f(0) \;\; f(1) \;\; f(2) \;\; f(3)\} = \{2 \;\; 1 \;\; 1 \;\; 1\}$$

in which $M = 4$. To test for evenness, the condition $f(x) = f(4-x)$ must be satisfied:

$$f(0) = f(4), \;\; f(1) = f(3), \;\; f(2) = f(2), \;\; f(3) = f(1).$$

Since $f(4)$ is outside the range being examined and it can be any value, the value of $f(0)$ is immaterial in the test for evenness.

The next three conditions are satisfied and the sequence is even.

In fact, any 4-point even sequence has to have the form $\{a \;\; b \;\; c \;\; b\}$.

According to (4.6-10b), the first term of an odd sequence, $w_o(0,0)$, is always 0. Consider the 1-D sequence

$$g = \{g(0) \quad g(1) \quad g(2) \quad g(3)\} = \{0 \quad -1 \quad 0 \quad 1\},$$

which satisfies the condition $g(x) = -g(4-x)$.

Any 4-point odd sequence has the form $\{0 \quad -b \quad 0 \quad b\}$.

The evenness and oddness of sequences depend also on the length of the sequences. For example, although $\{0 \quad -1 \quad 0 \quad 1\}$ is odd, the sequence $\{0 \quad -1 \quad 0 \quad 1 \quad 0\}$ is neither odd nor even.

The same basic considerations hold in 2-D. For example, the 6×6 2-D sequence

0	0	0	0	0	0
0	0	0	0	0	0
0	0	-1	0	1	0
0	0	-2	0	2	0
0	0	-1	0	1	0
0	0	0	0	0	0

is odd. However, adding another row or column of 0s would give a result that is neither odd nor even.

Now, we can establish a number of important symmetry properties of the DFT and its inverse.

The Fourier transform of a real function, $f(x,y)$, is conjugate symmetric:

$$F^*(u,v) = F(-u,-v). \qquad (4.6\text{-}14)$$

If $f(x,y)$ is imaginary, its Fourier transform is conjugate antisymmetric:

$$F^*(-u,-v) = -F(u,v)\,.$$

Table 4.1 lists symmetries and related properties of the DFT that are useful in digital image processing.

	Spatial Domain†		Frequency Domain†
1)	$f(x, y)$ real	$\Leftrightarrow$	$F^*(u, v) = F(-u, -v)$
2)	$f(x, y)$ imaginary	$\Leftrightarrow$	$F^*(-u, -v) = -F(u, v)$
3)	$f(x, y)$ real	$\Leftrightarrow$	$R(u, v)$ even; $I(u, v)$ odd
4)	$f(x, y)$ imaginary	$\Leftrightarrow$	$R(u, v)$ odd; $I(u, v)$ even
5)	$f(-x, -y)$ real	$\Leftrightarrow$	$F^*(u, v)$ complex
6)	$f(-x, -y)$ complex	$\Leftrightarrow$	$F(-u, -v)$ complex
7)	$f^*(x, y)$ complex	$\Leftrightarrow$	$F^*(-u - v)$ complex
8)	$f(x, y)$ real and even	$\Leftrightarrow$	$F(u, v)$ real and even
9)	$f(x, y)$ real and odd	$\Leftrightarrow$	$F(u, v)$ imaginary and odd
10)	$f(x, y)$ imaginary and even	$\Leftrightarrow$	$F(u, v)$ imaginary and even
11)	$f(x, y)$ imaginary and odd	$\Leftrightarrow$	$F(u, v)$ real and odd
12)	$f(x, y)$ complex and even	$\Leftrightarrow$	$F(u, v)$ complex and even
13)	$f(x, y)$ complex and odd	$\Leftrightarrow$	$F(u, v)$ complex and odd

TABLE 4.1 Some symmetry properties of the 2-D DFT and its inverse. $R(u, v)$ and $I(u, v)$ are the real and imaginary parts of $F(u, v)$, respectively. The term *complex* indicates that a function has nonzero real and imaginary parts.

†Recall that x, y, u, and v are *discrete* (integer) variables, with x and u in the range $[0, M - 1]$, and y, and v in the range $[0, N - 1]$. To say that a complex function is *even* means that its real *and* imaginary parts are even, and similarly for an odd complex function.

Example 4.11

Example 4.12

Fourier Spectrum and Phase Angle

Since the 2-D DFT is complex in general, it can be expressed in polar form:

$$F(u,v) = |F(u,v)|e^{j\phi(u,v)}, \qquad (4.6\text{-}15)$$

where

$$|F(u,v)| = [R^2(u,v) + I^2(u,v)]^{1/2} \qquad (4.6\text{-}16)$$

is the Fourier (frequency) spectrum, and

$$\phi(u,v) = \arctan\left[\frac{I(u,v)}{R(u,v)}\right] \qquad (4.6\text{-}17)$$

is the phase angle.

The power spectrum is defined as

$$P(u,v) = |F(u,v)|^2 = R^2(u,v) + I^2(u,v), \qquad (4.6\text{-}18)$$

where R and I are the real and imaginary parts of $F(u,v)$ and the discrete variables $u = 0,1,2,\ldots,M-1$ and $v = 0,1,2,\ldots,N-1$.

The spectrum has even symmetry about the origin

$$|F(u,v)| = |F(-u,-v)|, \qquad (4.6\text{-}19)$$

and phase angle has the odd symmetry about the origin

$$\phi(u,v) = -\phi(-u,-v). \qquad (4.6\text{-}20)$$

From the 2-D discrete Fourier transform defined in

$$F(u,v) = \sum_{x=0}^{M-1}\sum_{y=0}^{N-1} f(x,y)e^{-j2\pi(ux/M+vy/N)} \qquad (4.5\text{-}15)$$

we have

$$\begin{aligned} F(0,0) &= \sum_{x=0}^{M-1}\sum_{y=0}^{N-1} f(x,y) \\ &= MN\frac{1}{MN}\sum_{x=0}^{M-1}\sum_{y=0}^{N-1} f(x,y) \\ &= MN\bar{f}(x,y) \end{aligned} \qquad (4.6\text{-}21)$$

where $\bar{f}(x,y)$ denotes the average value of $f(x,y)$. Then, we have

$$|F(0,0)| = MN\left|\bar{f}(x,y)\right| \qquad (4.6\text{-}22)$$

Since the constant MN is usually large, $|F(0,0)|$ typically is the largest component of the spectrum (it could be several orders of magnitude larger than other terms).

$F(0,0)$ sometimes is called the *dc* component of the transform.

Example 4.13: The 2-D Fourier spectrum of a simple function

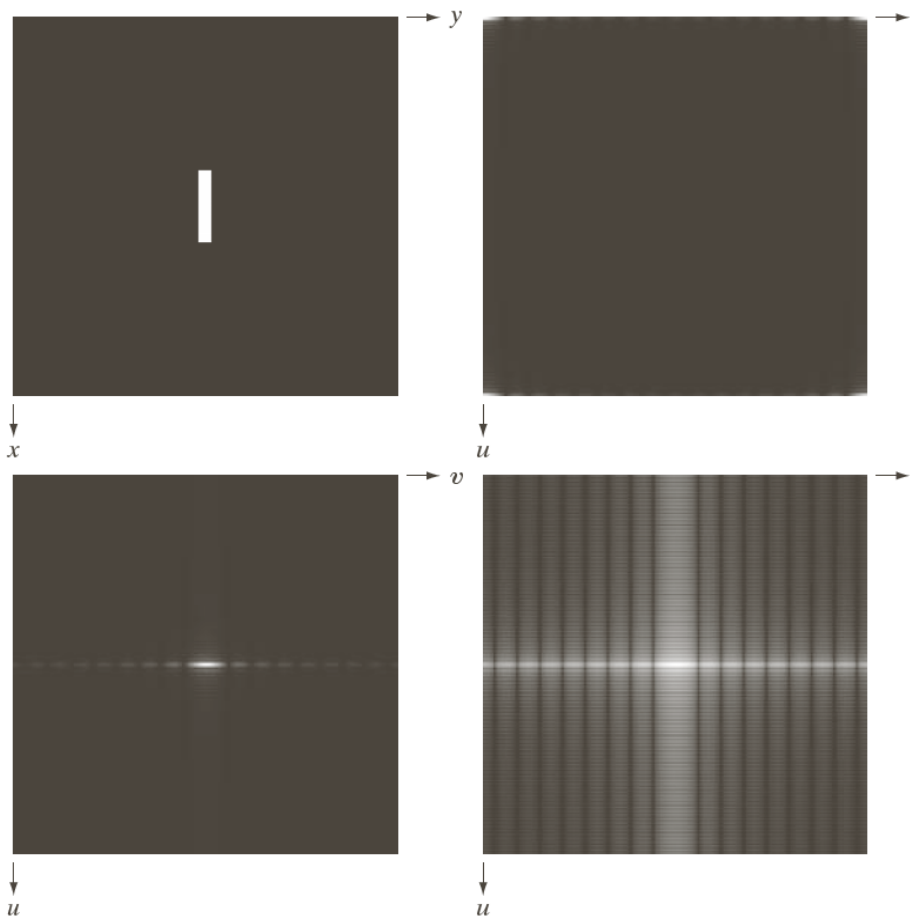

a b
c d

FIGURE 4.24
(a) Image.
(b) Spectrum showing bright spots in the four corners.
(c) Centered spectrum. (d) Result showing increased detail after a log transformation. The zero crossings of the spectrum are closer in the vertical direction because the rectangle in (a) is longer in that direction. The coordinate convention used throughout the book places the origin of the spatial and frequency domains at the top left.

Figure 4.24 (a) shows a simple image and Figure 4.24 (b) shows its spectrum, whose values were scaled to the range $[0,255]$ and displayed in the image form.

The origins of both the spatial and frequency domains are at the top left. Note that the four corners of the spectrum contain similarly high values. The reason is the periodicity property discussed in the previous section.

Figure 4.24 (c) shows the result of multiplying the image in Figure 4.24 (a) by $(-1)^{x+y}$ before computing the DFT.

Figure 4.24 (d) shows the display of $\log(1+|F(u,v)|)$. The increased rendition of detail is evident.

According to

$$f(x - x_0, y - y_0) \Leftrightarrow F(u,v)e^{-j2\pi(x_0u/M + y_0v/N)} \qquad (4.6\text{-}4)$$

and

$$f(r, \theta + \theta_0) \Leftrightarrow F(\omega, \varphi + \theta_0), \qquad (4.6\text{-}5)$$

the spectrum is insensitive to image translation (the absolute value of the exponential term is 1), but it rotates by the same angle of a rotated image. Figure 4.25 illustrates these properties.

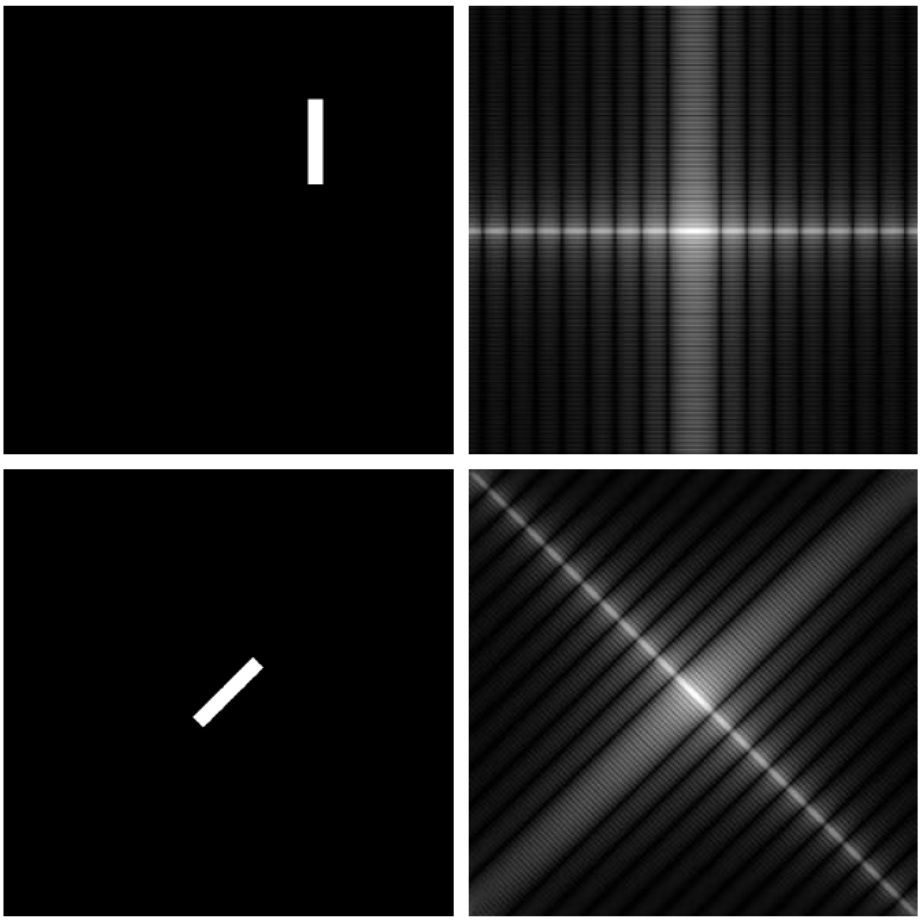

a b
c d

FIGURE 4.25
(a) The rectangle in Fig. 4.24(a) translated, and (b) the corresponding spectrum. (c) Rotated rectangle, and (d) the corresponding spectrum. The spectrum corresponding to the translated rectangle is identical to the spectrum corresponding to the original image in Fig. 4.24(a).

Figure 4.25 (a) shows that the rectangle in Figure 4.24 (a) was translated. Figure 4.25 (b) shows the corresponding spectrum, which is identical to the spectrum shown in Figure 4.24 (d). Figure 4.25 (c) and Figure 4.25 (d) are the images of rotated rectangle and the corresponding spectrum.

The images in Figure 4.24 (a) and Figure 4.25 (a) are different. If their Fourier spectra are the same, according to

$$F(u,v) = |F(u,v)|e^{j\phi(u,v)}, \qquad (4.6\text{-}15)$$

their phase angles must be different, as shown in Figure 4.26.

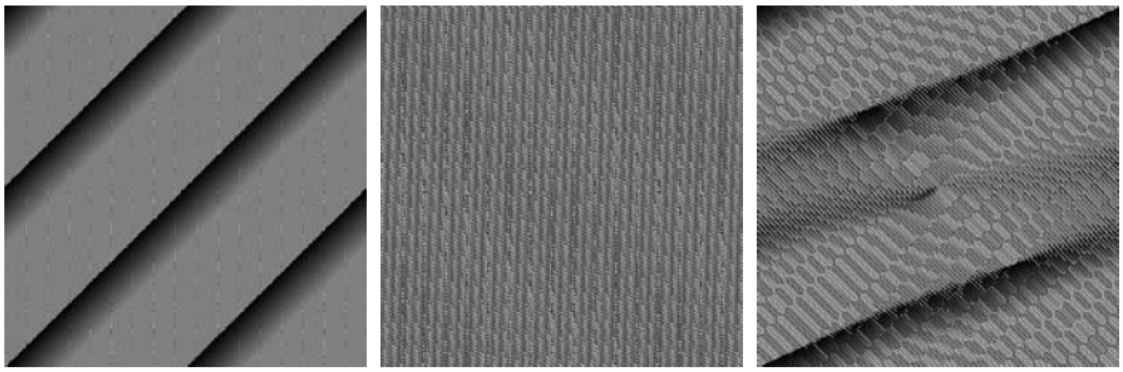

a b c

FIGURE 4.26 Phase angle array corresponding (a) to the image of the centered rectangle in Fig. 4.24(a), (b) to the translated image in Fig. 4.25(a), and (c) to the rotated image in Fig. 4.25(c).

Figure 4.26 (a) and Figure 4.26 (b) are the phase angle arrays of the DFTs of Figure 4.24 (a) and Figure 4.25 (a).

In general, visual analysis of phase angle images yields little intuitive information.

The components of the spectrum of the DFT would determine the amplitudes of the sinusoids that combine to form the resulting image.

At any given frequency in the DFT of an image, a large amplitude implies a greater prominence of a sinusoid of that frequency in the image. Conversely, a small amplitude implies that less of that sinusoid is present in the image.

The phase is a measure of displacement of the various sinusoids with respect to their origin.

Example 4.14: Further illustration of the properties of the Fourier spectrum and phase angle

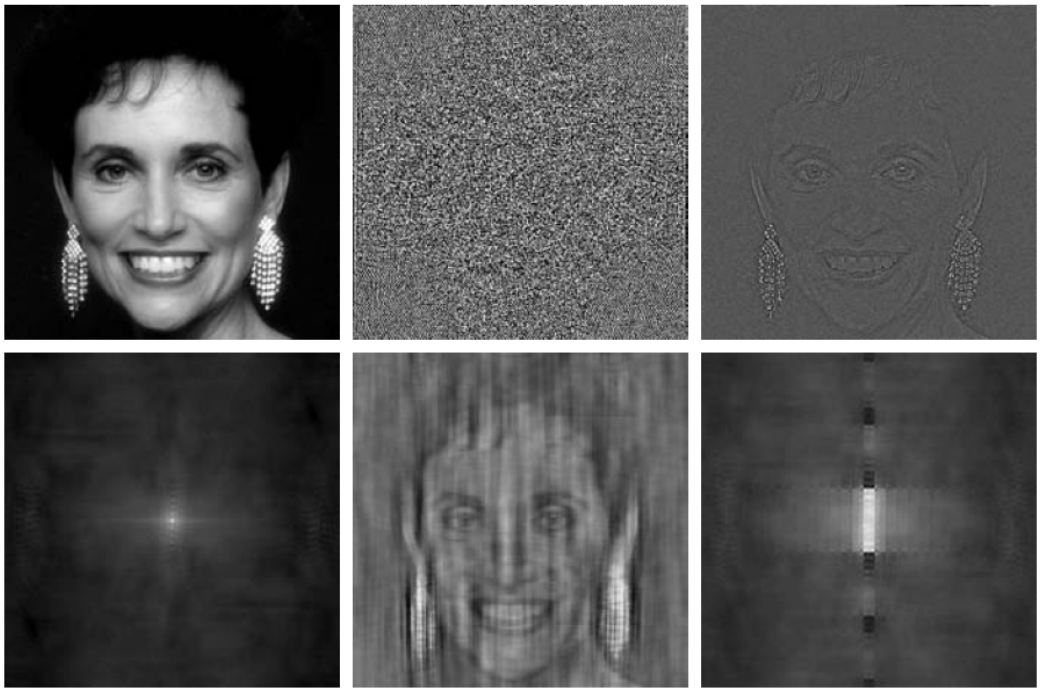

a b c
d e f

FIGURE 4.27 (a) Woman. (b) Phase angle. (c) Woman reconstructed using only the phase angle. (d) Woman reconstructed using only the spectrum. (e) Reconstruction using the phase angle corresponding to the woman and the spectrum corresponding to the rectangle in Fig. 4.24(a). (f) Reconstruction using the phase of the rectangle and the spectrum of the woman.

Figure 4.27 (b) is the phase angle of the DFT of Figure 4.27 (a).

Figure 4.27 (c) was obtained by computing the inverse DFT of

$$F(u,v) = |F(u,v)|e^{j\phi(u,v)} \qquad (4.6\text{-}15)$$

using only phase information. It shows the importance of the phase in determining shape characteristics.

Figure 4.27 (d) was obtained by using only the spectrum in (4.6-15) and computing the inverse DFT.

Figure 4.27 (e) and (f) show the dominance of the phase in determining the feature content of an image.

The 2-D Convolution Theorem

Extending

$$f(x) \star h(x) = \sum_{m=0}^{M-1} f(m)h(x-m) \qquad (4.4\text{-}10)$$

to two variables results in the expression for 2-D circular convolution:

$$f(x,y) \star h(x,y) = \sum_{m=0}^{M-1} \sum_{n=0}^{N-1} f(m,n)h(x-m,y-n) \qquad (4.6\text{-}23)$$

for $x = 0,1,2,\ldots,M-1$ and $y = 0,1,2,\ldots,N-1$. As in (4.4-10), (4.6-23) gives one period of a 2-D periodic sequence.

The 2-D convolution theorem is given by the expressions

$$f(x,y) \star h(x,y) \Leftrightarrow F(u,v)H(u,v) \qquad (4.6\text{-}24)$$

and, conversely,

$$f(x,y)h(x,y) \Leftrightarrow F(u,v) \star H(u,v) \qquad (4.6\text{-}25)$$

where F and H are obtained from using the 2-D discrete Fourier transform

$$F(u,v) = \sum_{x=0}^{M-1} \sum_{y=0}^{N-1} f(x,y)e^{-j2\pi(ux/M+vy/N)}. \qquad (4.5\text{-}15)$$

As mentioned previously, the double arrow, $\Leftrightarrow$, is used to indicate that the left and right sides of the expressions constitute a Fourier transform pair.

Equation (4.6-24) is the foundation of linear filtering, and is the basis for all the filtering techniques discussed in this chapter.

Figure 4.28 shows a 1-D example.

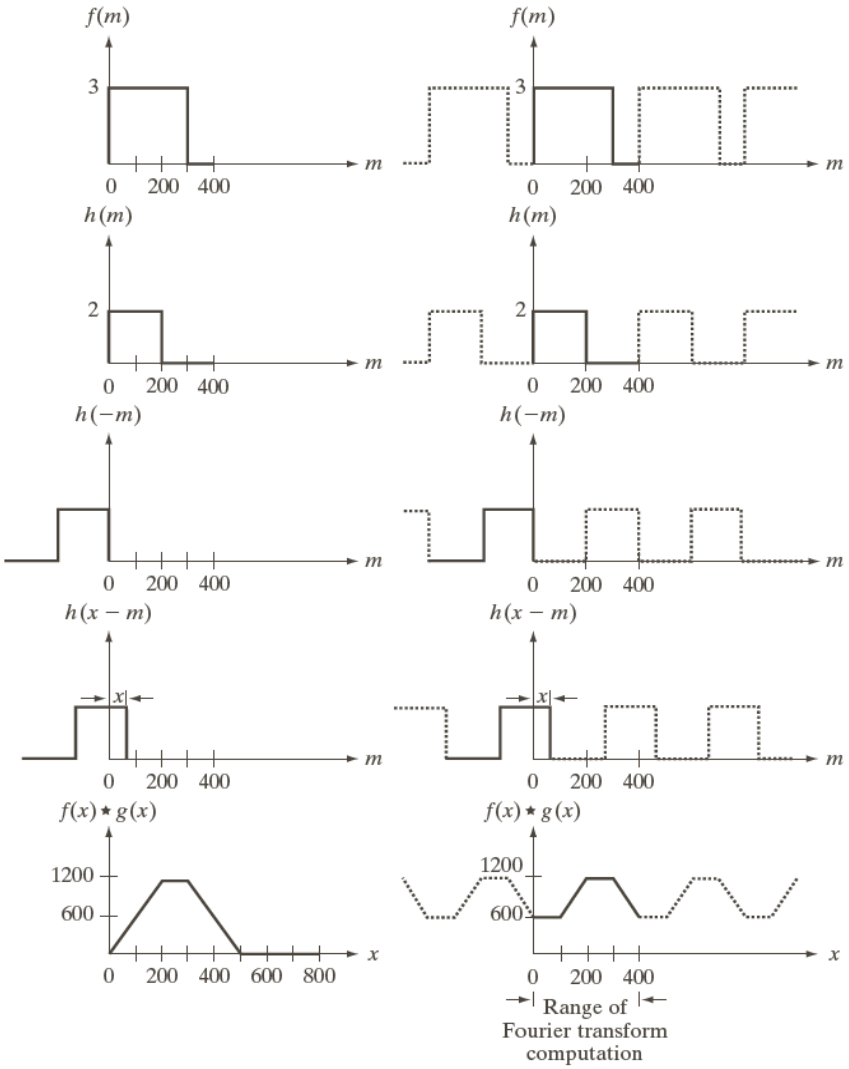

a f
b g
c h
d i
e j

FIGURE 4.28 Left column: convolution of two discrete functions obtained using the approach discussed in Section 3.4.2. The result in (e) is correct. Right column: Convolution of the same functions, but taking into account the periodicity implied by the DFT. Note in (j) how data from adjacent periods produce wraparound error, yielding an incorrect convolution result. To obtain the correct result, function padding must be used.

The left column of Figure 4.28 implements convolution of two functions, f and h, using the 1-D equivalent of

$$w(x,y)\star f(x,y) = \sum_{s=-a}^{a}\sum_{t=-b}^{b} w(s,t)f(x-s,y-t), \qquad (3.4\text{-}2)$$

which is

$$f(x)\star h(x) = \sum_{m=0}^{399} f(x)h(x-m).$$

Figure 4.28 (e) shows the convolution of these two functions.

If we use the DFT and the convolution theorem to obtain the same result as in the left column of Figure 4.28, we must take into account the periodicity inherent in the expression of DFT.

Figure 4.28 (f) and (g) are two periodic functions. Processing convolution with these two functions would yield the result shown in Figure 4.28 (j), which is incorrect. They interfere with each other to cause the so-called wraparound error.

To solve the wraparound error problem, consider two functions, $f(x)$ and $h(x)$ composed of A and B samples. If we append zeros to both functions so that they have the same length, P, then wraparound is avoided by choosing

$$P \geq A + B - 1 . \qquad (4.6\text{-}26)$$

In the example shown in Figure 4.28, each function has 400 points, so the minimum value we could use is $P = 799$. We can achieve that by appending 399 zeros to the trailing edge of each function. This process is called zero padding.

We would have the same conclusion regarding to wraparound error in 2-D. let $f(x, y)$ and $h(x, y)$ be two image arrays of sizes $A \times B$ and $C \times D$ pixels. Wraparound error in their circular convolution can be avoided by padding these functions with zeros, as follows:

$$f_p(x, y) = \begin{cases} f(x, y) & 0 \leq x \leq A - 1 \quad \text{and} \quad 0 \leq y \leq B - 1 \\ 0 & A \leq x \leq P \quad \text{or} \quad B \leq y \leq Q \end{cases} \qquad (4.6\text{-}27)$$

and

$$h_p(x,y) = \begin{cases} h(x,y) & 0 \le x \le C-1 \quad \text{and} \quad 0 \le y \le D-1 \\ 0 & C \le x \le P \quad \text{or} \quad D \le y \le Q \end{cases} \tag{4.6-28}$$

with

$$P \ge A + C - 1 \tag{4.6-29}$$

and

$$Q \ge B + D - 1 . \tag{4.6-30}$$

The resulting padded images are of size $P \times Q$. If both arrays are of the same size, $M \times N$, then we require that

$$P \ge 2M - 1 \tag{4.6-31}$$

and

$$Q \ge 2N - 1 . \tag{4.6-32}$$

As a rule, DFT algorithms tend to execute faster with arrays of even size, so it is a good practice to select P and Q as the smallest even integers that satisfy the above equations.

If the two arrays are the same size, P and Q are selected as twice the array size.

Summary of 2-D Discrete Fourier Transform Properties

TABLE 4.2
Summary of DFT definitions and corresponding expressions.

Name	Expression(s)
1) Discrete Fourier transform (DFT) of $f(x, y)$	$F(u, v) = \sum_{x=0}^{M-1} \sum_{y=0}^{N-1} f(x, y) e^{-j2\pi(ux/M + vy/N)}$
2) Inverse discrete Fourier transform (IDFT) of $F(u, v)$	$f(x, y) = \frac{1}{MN} \sum_{u=0}^{M-1} \sum_{v=0}^{N-1} F(u, v) e^{j2\pi(ux/M + vy/N)}$
3) Polar representation	$F(u, v) = \lvert F(u, v)\rvert e^{j\phi(u,v)}$
4) Spectrum	$\lvert F(u, v)\rvert = \left[R^2(u, v) + I^2(u, v)\right]^{1/2}$ $R = \text{Real}(F); \quad I = \text{Imag}(F)$
5) Phase angle	$\phi(u, v) = \tan^{-1}\left[\frac{I(u, v)}{R(u, v)}\right]$
6) Power spectrum	$P(u, v) = \lvert F(u, v)\rvert^2$
7) Average value	$\bar{f}(x, y) = \frac{1}{MN} \sum_{x=0}^{M-1} \sum_{y=0}^{N-1} f(x, y) = \frac{1}{MN} F(0, 0)$

(Continued)

Name	Expression(s)
8) Periodicity (k_1 and k_2 are integers)	$F(u, v) = F(u + k_1M, v) = F(u, v + k_2N)$ $= F(u + k_1M, v + k_2N)$ $f(x, y) = f(x + k_1M, y) = f(x, y + k_2N)$ $= f(x + k_1M, y + k_2N)$
9) Convolution	$f(x, y) \star h(x, y) = \sum_{m=0}^{M-1} \sum_{n=0}^{N-1} f(m, n) h(x - m, y - n)$
10) Correlation	$f(x, y) \star h(x, y) = \sum_{m=0}^{M-1} \sum_{n=0}^{N-1} f^*(m, n) h(x + m, y + n)$
11) Separability	The 2-D DFT can be computed by computing 1-D DFT transforms along the rows (columns) of the image, followed by 1-D transforms along the columns (rows) of the result. See Section 4.11.1.
12) Obtaining the inverse Fourier transform using a forward transform algorithm.	$MNf^*(x, y) = \sum_{u=0}^{M-1} \sum_{v=0}^{N-1} F^*(u, v) e^{-j2\pi(ux/M + vy/N)}$ This equation indicates that inputting $F^*(u, v)$ into an algorithm that computes the forward transform (right side of above equation) yields $MNf^*(x, y)$. Taking the complex conjugate and dividing by MN gives the desired inverse. See Section 4.11.2.

Name	DFT Pairs
1) Symmetry properties	See Table 4.1
2) Linearity	$af_1(x, y) + bf_2(x, y) \Leftrightarrow aF_1(u, v) + bF_2(u, v)$
3) Translation (general)	$f(x, y)e^{j2\pi(u_0x/M + v_0y/N)} \Leftrightarrow F(u - u_0, v - v_0)$ $f(x - x_0, y - y_0) \Leftrightarrow F(u, v)e^{-j2\pi(ux_0/M + vy_0/N)}$
4) Translation to center of the frequency rectangle, $(M/2, N/2)$	$f(x, y)(-1)^{x+y} \Leftrightarrow F(u - M/2, v - N/2)$ $f(x - M/2, y - N/2) \Leftrightarrow F(u, v)(-1)^{u+v}$
5) Rotation	$f(r, \theta + \theta_0) \Leftrightarrow F(\omega, \varphi + \theta_0)$ $x = r\cos\theta \quad y = r\sin\theta \quad u = \omega\cos\varphi \quad v = \omega\sin\varphi$
6) Convolution theorem†	$f(x, y) \star h(x, y) \Leftrightarrow F(u, v)H(u, v)$ $f(x, y)h(x, y) \Leftrightarrow F(u, v) \star H(u, v)$

(*Continued*)

Name	DFT Pairs
7) Correlation theorem†	$f(x, y) \star h(x, y) \Leftrightarrow F^*(u, v)\,H(u, v)$ $f^*(x, y)h(x, y) \Leftrightarrow F(u, v) \star H(u, v)$
8) Discrete unit impulse	$\delta(x, y) \Leftrightarrow 1$
9) Rectangle	$\text{rect}[a, b] \Leftrightarrow ab\dfrac{\sin(\pi ua)}{(\pi ua)}\dfrac{\sin(\pi vb)}{(\pi vb)}e^{-j\pi(ua+vb)}$
10) Sine	$\sin(2\pi u_0x + 2\pi v_0y) \Leftrightarrow$ $j\dfrac{1}{2}\left[\delta(u + Mu_0, v + Nv_0) - \delta(u - Mu_0, v - Nv_0)\right]$
11) Cosine	$\cos(2\pi u_0x + 2\pi v_0y) \Leftrightarrow$ $\dfrac{1}{2}\left[\delta(u + Mu_0, v + Nv_0) + \delta(u - Mu_0, v - Nv_0)\right]$

The following Fourier transform pairs are derivable only for continuous variables, denoted as before by t and z for spatial variables and by μ and ν for frequency variables. These results can be used for DFT work by sampling the continuous forms.

12) *Differentiation* (The expressions on the right assume that $f(\pm\infty, \pm\infty) = 0$.)	$\left(\dfrac{\partial}{\partial t}\right)^m\left(\dfrac{\partial}{\partial z}\right)^n f(t, z) \Leftrightarrow (j2\pi\mu)^m(j2\pi\nu)^n F(\mu, \nu)$ $\dfrac{\partial^m f(t, z)}{\partial t^m} \Leftrightarrow (j2\pi\mu)^m F(\mu, \nu); \dfrac{\partial^n f(t, z)}{\partial z^n} \Leftrightarrow (j2\pi\nu)^n F(\mu, \nu)$
13) *Gaussian*	$A2\pi\sigma^2 e^{-2\pi^2\sigma^2(t^2+z^2)} \Leftrightarrow Ae^{-(\mu^2+\nu^2)/2\sigma^2}$ (A is a constant)

†Assumes that the functions have been extended by zero padding. Convolution and correlation are associative, commutative, and distributive.

TABLE 4.3
Summary of DFT pairs. The closed-form expressions in 12 and 13 are valid only for continuous variables. They can be used with discrete variables by sampling the closed-form, continuous expressions.